# Direct Ink Writing of Mineral Materials —A review

Liang Hao[1,3], Danna Tang[1,3,#], Tao Sun[2], Wei Xiong[1,3], Zuying Feng[3], Ken E Evans[4], Yan Li[1,3,#]

1 Gemological Institute, China University of Geosciences, Wuhan, 430074, P. R. China
2 Engineering College, China University of Geosciences, Wuhan, 430074, P. R. China
3 Advanced manufacturing center, China University of Geosciences, Wuhan, 430074, P. R. China
4 College of Engineering, Mathematics and Physical Sciences,, University of Exeter, Exeter, EX4 4QJ, UK
# Corresponding Author / E-mail: dana.cug@foxmail.com
# Corresponding Author / E-mail: yanli@cug.edu.cn

KEYWORDS: Additive Manufacturing, Slurry Deposition, Mineral Materials, Physical and Chemical Properties, Processing Methods

*Due to the intrinsically limited mechanical properties, functionalities and structures of mineral materials made through traditional fabrication approaches, there is a critical need to develop new 3D forming techniques that can construct mineral composite materials and their structures with high performance and functionalities. The Direct Ink Writing (DIW) approach offers many advantages in the fabrication of mineral materials composites, including high precision, cost effectiveness, customized geometry and environmental friendliness. This review gives a comprehensive overview on the state of the art of DIW mineral materials, including materials classification, preparation and properties. It presents the critical steps for processing mineral materials and their effects on the properties and performance of mineral materials. In addition, the applications of DIW in the fields of architecture, tissue engineering, functional micro parts and geological engineering modelling are presented.*

**NOMENCLATURE**

DIW = direct ink writing
AM = additive manufacturing
3D = three−dimensional
2D = two−dimensional
MMC = Mineral Material Composites

## 1. Introduction

Direct ink writing (DIW) utilizes a flowable binder or colloidal slurry highly loaded with powder particles to form 3D shapes via additive manufacturing (AM). Direct ink writing (DIW) is an extrusion-based printing technique. Viscous materials like solutions, hydrogels and pastes are extruded through nozzles by the force of a piston, a screwing system, or pneumatic pressure.[1-4] Initially, it was primarily used to fabricate ceramic parts as the ceramic slurry can be loaded to ahigh density compared to a dry powder before sintering. Due to its unique flexibility and capacity for a highvolume loading of micro or nano particles which are hard to be handled by other powder-based AM processes such as selective laser sintering or melting, DIW has gradually extended its applications to metal and polymer composites. Hence, this technique demonstrates feasibilities to process different combinations of various material powder and binders, with a wide variety of applications.

The DIW process also offers specific unique advantages for the special personalized precision and complex parts. First, the manufacture of high−precision parts meets the needs of many industries, such as micro−scale cell printing in bio-printing.[5] Second, complex shapes especially pore structures can be fabricated relatively easily with DIW, whereas conventional methods are limited to the fabrication of parts with two−dimensional (2D) and simple three−dimensional (3D) geometries.[6] Third, the combined high−precision and complex structure could achieve better manipulation of physical or chemical properties that are difficult to obtain using conventional processes.

The attractive features of the DIW process can be applied advantageously to the fabrication of mineral materials (**Fig. 1**). Although these mineral materials offer unique properties that cannot be normally achieved in traditional synthetic composites, its broad applications are often restricted by their flexible structural design. The adoption of DIW of mineral material offers a potential of achieving the special physical and chemical properties of mineral materials. In recent years, a few pioneering researches have been conducted to investigate the feasibility of DIW for the fabrication of mineral material composites.[7, 8] The most widely studied mineral material composites are used for structural reinforcement and functional device with a scope of offering good mechanical and chemical properties.[9, 10] Theoretically it might be possible to use a variety of mineral materials for different performance enhancements, however, the synergistic control of mineral material and structure could face a number of uncertainties. In reality, mineral material composites are often used to achieve only one

or two performance enhancements. At the same time, micro-nano mineral printing and gradient printing have been used in many applications with the development of DIW technology.[11-15] In the end,

**Fig. 1** The attractive features of the DIW process applied to the fabrication of mineral material

there will be many advantages, especially in terms of precision si mulation and environmental friendliness.[16-18]The main purpose of this review paper is to give a comprehensiv e picture of the current state of the art on DIW of mineral material composites. This paper provides a review of processing technologi es related to composite fabrication through the DIW route. It also

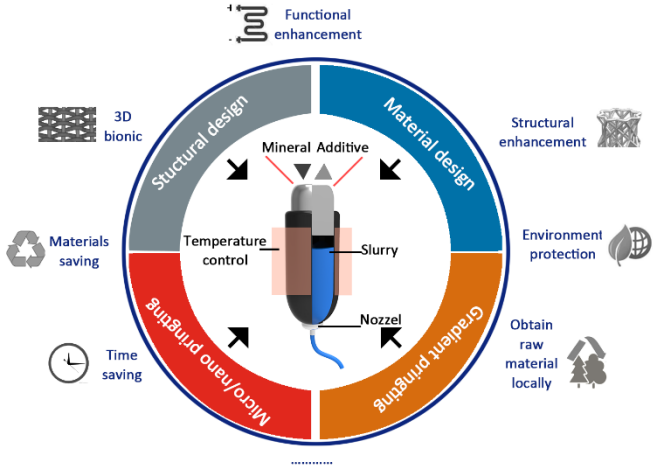


presents the main applications of deposition−based 3D printed mi neral material composites. Furthermore, further research direction on DIW of mineral material composites is also discussed.

## 2. Mineral materials

The many mineral materials are manufactured from naturally occurring rock. Mineral materials are mainly divided into physically enhanced (Structural materials) and chemically enhanced materials (Functional materials). Structural mineral materials are mainly used in manufacturing and construction industries. For instance, vermiculite, pumice, volcanic slag, perlite, and expanded shale can be used to make lightweight construction materials that contain a large number of pores, and have thermal insulation properties.[19] Functional mineral materials are mainly used in the electronics, lasers and instrumentation industries. For example, quartz is used as a resonator, as a frequency standard, in an electronic watch.[20]

When DIW is applied to a mineral material, the refined mineral powder is melted together with the additive to achieve high precision forming. For uniform performance, mineral materials need to be evenly dispersed and meet the millimeter/ nanometer level of printing. Slurry can be obtained using additives to achieve suspension of the mineral powder, the quality of the mineral dispersion in the matrix composites slurry could significantly affects the final properties of the composite.

The published papers on mineral material composites reveal that the main challenge has been to produce good quality mineral material composites with required performance. Typically, certain mineral materials are used only for one type of performance enhancement because it is difficult to achieve when multiple performance enhancements are required, which is particularly evident in mineral material models.[21] So the studies associated with material formulation focus on the development of processing routes that could produce good dispersion of mineral material composites.[22, 23] In addition, a number of research groups also investigated the performance optimization and structural design of mineral materials, indicating that the mineral powder and slurry preparation plays important roles on the performance of mineral materials.[24, 25] It is hoped that many kinds of efficient design of composites can reduce experimental repeatability and improve manufacturing efficiency.[26, 27]

### 2.1 Mineral powder

The choice and proportion of mineral powder has direct effects on the forming of mineral material composites and the properties and performance of the mixed mineral material composites. Acting as the filler material, the mineral powder is normally deagglomerated using various methods including conventional ball milling or high-energy ball milling methods, and then mixed with additives to produce slurry of well dispersed mineral material composites.

When varieties of mineral materials are combined, the particle size and content of the mineral have a significant effect on the structure and its properties. The selection of mineral materials should consider the both characteristics of each mineral material as well as the mixtures.[28] The mixing of many different types of mineral powder would give better results, so the properties of the powder itself and the properties after mixing need to be considered. Schulten et al. believed that the precise description of mineral particles could help in quantifying its impact on the properties.[29] Halit et al. investigated microstructures of different mineral powder mixtures under different curing conditions.[30] Therefore, micro or nano-scale fine mineral powder will bring better performance. Puget et al. also found that microaggregates of mineral mate (<200 μm) were more stable than large aggregates (>200 μm), thus the design of particles and components plays a decisive role in the performance of the slurry.[31]

The particular characteristics of mineral material powder depend on its microstructure. The research reported so far has proved that the special structure of mineral materials plays a crucial role in nature and facilitates the exertion of chemical effects.[32] The common octahedral and tetrahedral structures of many mineral material powders reveal the causes of their particular characteristics. Because the physical properties of tetrahedron and octahedron are more stable, and they perform better in energy conversion and transmission such as light, magnetism, electricity, heat and sound.

The combination of different mineral materials can produce a variety of forms with the enhanced properties. Mineral fiber structure is widely used for properties enhancement as summarized in **Table 1**. The study on the structure of mineral materials shows that the mixed combination of various mineral powder particles could lead to strong bending and tensile properties.[33] The inclusion of fiber mineral materials can enhance performance in a variety of mineral shape tests (angular, cubical and elongated shapes). In particular, the aligned discontinuous mineral fiber can effectively enhance mechanical properties, including compression, bending and toughness performances of its mineral material composites.[34] Besides, Tai et al. investigated peak strains of mineral mixtures containing different fiber strengths.[35] Mineral composite materials have also demonstrated

superior performance and environmental protection as friction materials.[36] The functional enhancement of many kinds of natural material is designed to effectively reduce environmental pollution, especially in the use of materials in situ which can reduce time and transportation costs.[37]

**Table 1** Mineral powder at different level and their improved properties

| Content | Mineral powder | Enhancement in properties | Ref. |
|---|---|---|---|
| Mineral composites (25 wt. %) | Silica fume<br>Limestone<br>Ultra-fine gypsum | Optimize the properties of slump, unit weight, air entrancement, compressive strength, tensile strength, flexural strength and modulus of elasticity | [38] |
| Silica Fume (10 wt. %),<br>Fly ash (20 wt. %)<br>Sugarcane Bagasse Ash (10 wt. %) | Silica Fume (SF),<br>Fly ash (FA)<br>Sugarcane Bagasse Ash (SCBA) | Improve permeable voids,<br>water absorption, initial rate and abrasion resistance | [39] |
| Basalt and ceramic composites with different fibers (5, 15, and 25 wt. %). | Basalt<br>Ceramic | Strengthen tensile and flexural strength, stiffness and fracture toughness | [9, 34] |
| SiO2 (≥26.0 wt. %)<br>Na2O (≥8.2 wt. %) | Basalt fiber | Improve both the yielding and the ultimate strength of the beam specimen up to 27% | [40, 41] |
| Fine aggregate (55 wt. %)<br>Coarse aggregate (40 wt. %)<br>Fine sand (5 wt. %) | Silica fume<br>Fly ash<br>Silica fume | Increase fresh density, compressive, splitting and flexural strengths | [22] |
| - | Class-C fly ash (FA) Ground granulated blast furnace slag (GGBFS) | Strengthen mechanical properties (compressive strength, flexural strength, and toughness) | [30] |
| - | Mineral fibers on the basis of basalt and ash and slag waste | Increase corrosion resistance<br>, physical-mechanical and performance characteristics | [23] |

### 2.2 Various binder additives

Additive processing is a technique for producing mineral suspensions on the basis of colloidal chemistry. This technique is used to prepare mineral material composites by combining a variety of additive binders and mineral powders. For the same mineral material, the additive binders can be different depending on the post−processing needs. Typically, the slurry suspensions are mixed slowly by magnetic stirring ultrasonication in order to obtain uniform distribution of the additive into the mineral powder.

The slurry can be in the form of a solution, a suspension, a colloid, or the like and the same kind of mineral material applies a variety of additive types. The most common additive binder systems for Metal Injection Molding (MIM) and Ceramic Injection Molding (CIM) are thermoplastic system and water−soluble system.[42-45] In order to meet the requirements, the mixture of multi−component additives is normally used.[46] The choice of additives for mineral materials is more extensive based on the application. **Table 2** summarizes the binder used by mineral material and made a simple classification. It is divided into two types based on whether additives need to be removed. In some cases, additive binders do not require post−treatment removal, such as geological engineering model and biological tissue applications.[47, 48] On the other hand, the additives that are required of post-treatment removal are mostly wax−based additives and water−based additives.

**Table 2** The binder used by mineral material and its classification

| Type | Binder | Content | Ref. |
|---|---|---|---|
| polymer binder | Resin binder;<br>Phenol-Urea-Formaldehyde (PUF) binder;<br>Alkanol amine- acid anhydride binder | Formaldehyde to<br>Phenol (3.5-3.9 mol. %);<br>Urea to phenol (1.5-2.5 mol. %) | [49, 50] |
| Wax-based binder | Oxidized paraffin wax | Gradient change test | [51, 52] |

| | | | |
|---|---|---|---|
| Solvent binder | An ether solvent-based binder (ExOne PM - B - SR1 - 04) | Gradient change test | 53 |
| Aqueous binder | A sugar syrup;<br>A polycarboxylic acid;<br>An amine;<br>Areaction product of a polycarboxylic acid component and an amine | The sugar syrup<br>(at least 55 and less than 80) | 54 |

The selection of the various additives depends on the application requirements, of which wax−based additives are the most common type of additive shown in **Fig. 2**. [8] This kind of formulation is very similar to the suspensions used for ceramic injection moulding which are primarily composed of ceramic powders and wax-based organic matrix, and then sintering produced multi-structural and multi-functional ceramics.[55-57] Kafara et al. investigated the influence of binder quantity on dimensional accuracy and resilience in 3D Printing.[58] It could be seen in **Fig. 3** that binder quantity had great effect on the three-point bending curling results and geometric deviation of the 3D Printed specimens made of wax−based materials. As the amount of additive increased, the bending strength increases almost linearly, and the same applies to compressive strengths up to 70% of the amount of additive. It appeared that the maximum curling as well at 70 wt. % binder saturation. Adjusting the drying process of the printed part could help to counter the curling. Meanwhile, additive saturation also has an effect on deviations. The more binder is, the more deviation is. Furthermore, wax−based additives also have a crucial impact on the performance of the 3D printing forming process, indicating that the more comprehensive study is required to illustrate the effect of additive quality and content on the 3D printing forming process as well as the performance of 3D printed final product.

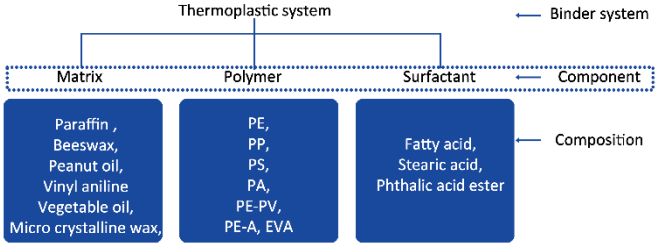


**Fig. 2** Three kinds of additive components in the thermoplastic system **Ref. 8**

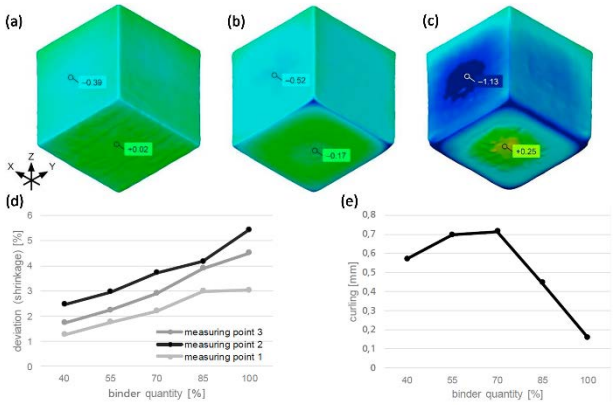


**Fig. 3** Deviation of the cubic specimens in comparison to the CAD fil e for the binder quantity (a) 40 %, (b) 75 % and (c) 100 %. (d) The de viations of the four cubic specimens' sides, which are arranged in par allels to the building direction (Zdirection), (e) Curling of the specime ns for the three-point bending test **Ref. 58**

The stability and fluidity of additives are the determining factors for successful DIW. In general, researchers have to estimate the physical, thermal ad rheological properties of the additives and it mixed

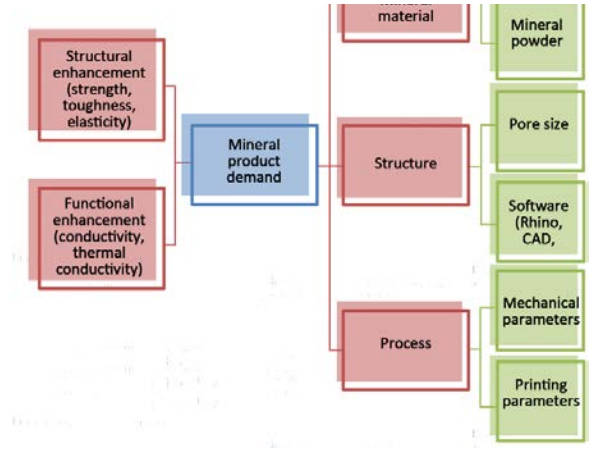


metal and ceramic powders.[59, 60] It is also a challenge to ensure that they do not exhibit delamination because many mineral material slurries are non−Newtonian fluids. Peltolaet al. extruded the mixed mineral slurry in a screw way rather than the usual injection extrusion.[61] This could lead to the increased viscosity and consistency of mineral materials and their colloids and plastic additives. This would require the specific mineral material to maintain high viscosity and stability in the condition of greater extrusion force. Colloids and plastic additives can increase viscosity to achieve consistency of mineral materials.

## 3. Processing routes for dispersion slurry

Another important aspect associated with the preparation of mineral powder and slurry paste is to ensure the processing routes that could lead to the good dispersion of mineral powder within the paste, and the whole printing process is as shown in **Fig. 4**. The quality of the mineral powder dispersion in the paste could significantly affect the final properties of the composite. In the past decade, there has been a

considerable amount of work to produce well-dispersed mineral composites for AM application. Due to its capability of using diversified mineral materials and slurry binders, DIW represents as a very flexible AM technique with relatively shortened material and process development cycle. The recent papers published in the field of DIW of mineral material composites show that many researchers work on the process improvement and optimization of DIW. The processing parameter setting and adjustment are the key research areas.

**Fig. 4** The whole process of printing mineral materials

### 3.1 Advantages of mineral DIW process

In the past, the processing of mineral materials was mostly manual, especially in the construction and other industries.[62] Gradually, the artificial processing of mineral materials adopts machinery. Slow pouring and two−dimensional automated processing began to replace labor. The semi−automatic processing is also used to make some relatively small mineral products. Therefore, the three-dimensional structure processing of mineral materials began to use DIW process.

DIW is capable of depositing a fine line of highly loaded powder particle with its binder slurry. It posts less strict requirement of powder particles in term of specific form, shape or sizes. Broad selection of various mineral materials could be formed into different specifications for the intended use. Especially, it can use powder particles in micro or nano size, offering better functionality or densities after post sintering process. Therefore, it has better versatility and adaptability in term of material range in comparison with other AM processes such as powder based selective laser sintering or melting process. This offers its broad application in the field of tissue engineering scaffolds, functionally graded materials, functional electronic devices, and functional ceramic devices.

Hence, DIW offers specific advantages for both scientific research and commercial over other 3D printing methods. Currently, 3D printing processes are generally classified according to the type of materials and the layer consolidation approaches. As can be seen in **Table 3**, these 3D printing technologies advocated by different companies demonstrates different level of material range. Among them, DIW technology has the greatest compatibility with almost all powder materials. This would offer great potential of fabricating mineral materials.

**Table 3** 3D printing technology classification

| Types | Technology categories | Printable materials | Energy consumption | Ref. |
|---|---|---|---|---|
| Extrusion forming | Fused Deposition Modeling (FDM) | Thermoplastic, Fused metal, Edible material | Middle | 63-65 |
| | **Direct ink writing (DIW)** | **Almost all powder materials** | **Low** | **{Sun, 2015 #164}** |
| Granular material forming | Direct Metal Laser Sintering (DMLS) | Almost any metal alloy | High | 66 |
| | Electron Beam Melting (EBM) | Titanium alloy | High | 67 |
| | Selective heat sintering (SHS) | Thermoplastic powder | High | 68 |
| | Selective Laser Sintering (SLS) | Thermoplastics, metal Powders, ceramic Powders | High | 69-71 |
| | 3D printing based on powder bed, nozzles and plaster (PP) | plaster | Middle | 72 |
| Photopolymerization forming | Stereolithography Apparatus (SLA) | Photopolymer | Low | 73 |
| | Digital Light Processing (DLP) | Liquid resin | Low | 74 |
| Lamination forming | Laminated Object Manufacturing (LOM) | Paper, metal foil, ceramic | Middle | 62, 75, 76 |

The artificial processing of mineral materials has beengradually replaced by machinery. In the past, the processing of mineral materials was mostly manual, especially in the construction and other industries.[77] Slow pouring and two-dimensional automated processing began to replace labor. The processing of some relatively small products also belongs to semi-automatic processing. However, the performance of three-dimensional structure has given rise to the need for three-dimensional processing of mineral materials. This has caused

a lot of changes in the industry, and has achieved remarkable results in the fields of construction and medical care.[78-81]

### 3.2 Process parameters control in DIW

There are many parameters in mineral material slurry control, the adjustment of parameters is directly related to the status of the slurry. The parameter control of DIW of is less controllable than other forming methods due to the flexibility of its manufacturing method. However, whether or not warming determines the main control parameters of DIW due to the difference in mineral material slurry morphology.

Heating controlled mineral materials are used in more sophisticated applications, so micropore print nozzle related parameters are the focus of research. First, the control of extrusion flow is a universal issue in the DIW of various materials. Woodfield et al. achieved gaps of 1 mm and 71% porosity of mineral bone scaffold through microfluidic control.[82] In the course of this experiment, the parameters of the mineral material were experimentally adjusted, including parameters such as fiber deposition temperature and crosshead speed, resulting in alternating stent structures as shown in **Fig. 5**. Prior to this, experiments have also proved that this type of material had superior mechanical properties compared to other materials in the case of the same geometry.[83] Similarly, control of precursor flow helps the mineral battery achieve high crystallinity and electrochemical performances.[84, 85] Secondly, the temperature control of nozzle and heating bed are the key parameters. The material sticks when the temperature is too high, and the material is blocked when the temperature is too low.[86]

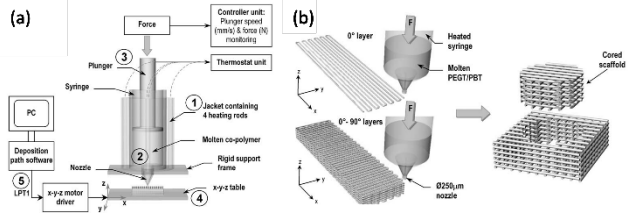


**Fig. 5** (a) The 3D deposition device consisted of five main components: (1) a thermostatically controlled heating jacket; (2) a molten co-polymer dispensing unit consisting of a syringe and nozzle; (3) a force-controlled plunger to regulate flow of molten co-polymer (4); a stepper motor driven x-y-z table; and (5) a positional control unit consisting of x-y-z stepper−motor drivers linked to a computing software that generates material deposition paths. (b) 3D deposition process where +250 mm PEGT/PBT fibers are successively laid down in a computer-controlled pattern (0−90°orientation shown). Scaffolds are subsequently cored from the deposited bulk material **Ref. 82**

Extrusion of mineral paste needs to balance extrusion force and fluid stability, requiring a better match between nozzle and extrusion rate, especially when the driving force is greater.[87] Mineral slurry stability system meets the DLVO theory, so mineral particles have hydration repulsion energy and are closely related to distance (**Equation 1**). The force between the particles increased when the distance reduced so that particle agglomeration can easily occur, which should try to be avoided. When pressure is applied, the liquid is forced to flow from the inter-particles to the pressure direction, so that large particles form an aggregate on the upper part of the syringe to form a deposit when the attraction of the particles is not enough. When pressure is applied, the aggregation rate due to diffusion in this force-field can be calculated by the Fuchs formula (**Equation 2**).[88-91] Particles will aggregate approximately with the diffusion controlled rate at high viscosity, since the van der Waals forces and hydrodynamic interactions have only minor effects. In addition, such printing is often faced with special circumstances such as Lossless weight and high pressure conditions which post higher demands on mineral materials and printing machinery.[92] Nair et al. proposed a series of strategic, technological and ethical aspects of establishing colonies on Moon and Mars.[93] Moon and Mars face a different situation from the earth like the surface features, in situ resources, and the dynamics of the planets like quakes, dust storms etc. In this respect the printing device has to be designed for specific planetary features.

$$V_{HR} = 2\pi \frac{R_1 R_2}{R_1+R_2} h_0 V_{HR}^0 \exp(-\frac{H}{h_0}) \cdots\cdots 1$$

Where $R_1$ and $R_2$ are the neighboring powder particle radius re spectively, $V_{HR}^0$ is the energy constant, $h_0$ is the attenuation leng th, $H$ is the Interaction distance.

$$k = \frac{2kT}{3\eta R_{eff}} [\int_0^\infty \frac{B(h)}{(R_+ + R_- + h)^2} \exp(\frac{U(h)}{K_B T}) dh]^{-1} \cdots\cdots 2$$

Where $k$ is the aggregation rate coefficient, $T$ is the absolute temperature, $\eta$ is the viscosity of paste, $R_{eff}$ is half the radius of R, $B(h)$ is the hydrodynamic resistance function, $R_+$ and $R_-$ are the radius of the two particles involved, $h$ is the surface separation, $U(h)$ is the interaction free energy of the two particles, $K_B$ is the Boltzmann constant.

### 3. 3 Micro/nano powder forming

Over the past few years, DIW of ultrafine particles has been a major research hot spot and development trend. Micron and

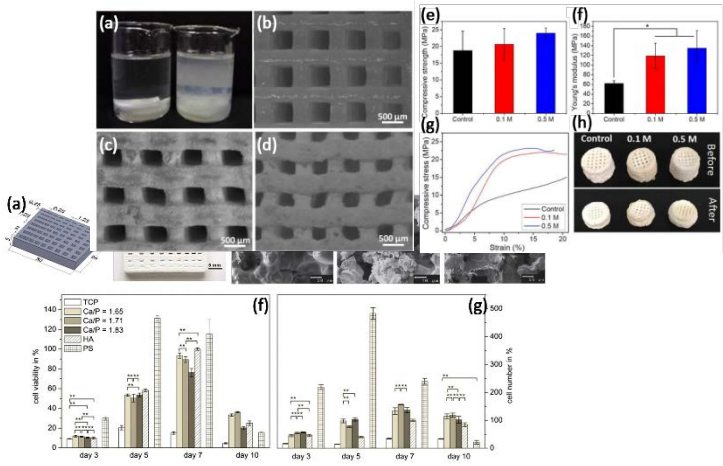


nanoparticle mineral powders exhibit unique superior properties, especially in the formation of microstructures and micropores. Therefore, there is a greater challenge for the process control of ultra-micro mineral particles. Fine print also imposes more requirements on the jet head.

In work done by Castilho et al., they showed micron-sized powders provide superior performance in micron-sized pores in the field of bone support manufacturing in **Fig. 6**.[94] Firstly, the designed powder system had the production of specimens with an accuracy of 500 μm and a minimal pore size of approximately 300 μm. The sintered cake was crushed with pestle and mortar and milled in a planetary ball mill and sieved <100 μm. This micron powder resulted in scaffolds with a dimensional accuracy of >96.5% and a minimal macro pore size of 300

μm, enhancing the ultimate compressive strength by a factor of 8 and the modulus of toughness by a factor of 4. Also, it showed a good cytocompatibility of BCP comparing with HA. The HA/TCP ratios of BCP scaffolds with a Ca/P ratio of 1.65 and 1.71 were almost inverse (Ca/P ratio = 1.65 with HA/TCP = 30/70). High-precision mineral powder composition for DIW offers an excellent method to produce individual bioactive bone implants.

**Fig. 6** (a) Design of macroporous plate to prove the printing accuracy. (b) The 3D printed plate shows an accuracy of 500 μm and a minimal pore size of 300 μm. SEM of a PLGA loaded printed and sintered BCP specimen. (a) The external surface of the specimen is covered with a homogeneous polymer coating, (b) without complete sealing of the pores. (c) The peripheral zone of the specimen shows a depth of impression of approximately 200 μm. (a) Cell viability and (b) cell proliferation of osteoblastic cells MG63 cultivated on printed pure TCP, pure HA, different BCP scaffolds and PS over a period of ten days. The phase composition affected the analyzed parameters cell viability and cell proliferation as evaluated by ANOVA test: ** = no significant difference (p-value > 0.05). The cells on BCP specimens showed an enhanced proliferation and viability virtually independent from the TCP/HA content compared to pure TCP **Ref. 94**

**Fig. 7** showed that Luo et al. used a similar method with a nano-scale apatite matrix.[95] This experiment controlled the thickness of the nano apatite scaffold by the amount of phosphate ions in the DIW. The stent with a uniform nano apatite scaffold had 2-fold higher Young's modulus compared to the scaffold without apatite. Furthermore, nano apatite scaffold significantly increased the protein adsorption on the surface of scaffolds. Accordingly, the bionic nano composite stent is a more superior choice for bone tissue engineering.

**Fig. 7** Photographs of 3D printed scaffolds soaking in $CaCl_2$ solution (a) without (0.1 M NaCl) (left) and with (0.1 M $Na_2HPO_4$) (right) mineralization; (b) Microscopic images of 3D printed alginate/ gelatin scaffolds with 0.1 M NaCl and with (c) 0.1 M $Na_2HPO_4$ and (d) 0.5 M $Na_2HPO_4$. Compressive strength (e), Young's modulus (f) and stress-strain curves (g) of 3D printed scaffolds with and without mineralization, and pictures of scaffolds before and after compression (h).0.1 M NaCl (control), 0.1 M $Na_2HPO_4$ (0.1 M), and 0.5 M $Na_2HPO_4$ (0.5 M). (*p<0.05, n=5) **Ref. 95**

Although the printing of micro/nano mineral materials has brought more superior physical and chemical properties, the real three-dimensional complex structure design still needs to be further improved for DIW technology. Recently, in Kokkinis's work, it is clear that hydrogel materials can achieve biological printing of complex structures of multiple materials, but the mineral materials of the bone scaffold are not yet to be printed in this way.[96] Though 2-component dispenser "preeflow eco-duo450" (ViscoTec GmbH) allows for printing of compositional gradients using two components mixed at predetermined ratios, the instrument is only used in biological printing and larger printing is still lacking.[97] Therefore, this kind of equipment is expected to be expanded in the printing of micro/nano mineral materials, laying a foundation for the further manufacture of complex and high performance mineral materials products.

## 4. Applications of DIW mineral material composites

The mineral materials will develop in the direction of energy saving, material saving and high performance. The DIW of mineral functional materials will occupy a more important position. Through the study of mineral physics, the directional design of mineral materials made with additives is an important part of the study of mineral materials in the future.

### 4.1 Architecture and out-space in habitation building application

With the need for mechanical strength and complex shape of the architecture, deposition-based 3D printed mineral material composites technology has become more mature with higher environmentally. Using the designed structure, printers can automatically print complex structures in various complex environments, especially the innovative realization of material self-circulation green manufacturing. Mineral material composites used for printing in the field of architecture applications are based on treated soil and rocks as well as binder. The desired traits of printable materials for architecture applications are printability, environmental-friendly, good mechanical properties and structural properties.

In order to meet the living requirements of the mechanical properties of the building structure, high-strength materials and structures have been deeply explored. For the study of mineral materials, it is necessary to prevent plastic deformation and have low yield strength of the material. Perrot et al. experimentally demonstrated that the strength of the mineral material composites must be sufficient to maintain the weight of the deposited layer.[98] Rangel et al. also proposed that the mineral materials viscosity needs to be sufficient to avoid dead ends.[99] Simultaneously, the clever design of the building structure results in greater mechanical strength and improved design. For example, the lightweight honeycomb structure composed of nano-clay plates achieved less material usage and greater pressure strength.[100] As a result, architectural printing can achieve higher height and environmental resistance.[101]

With more printing requirements for special environments,

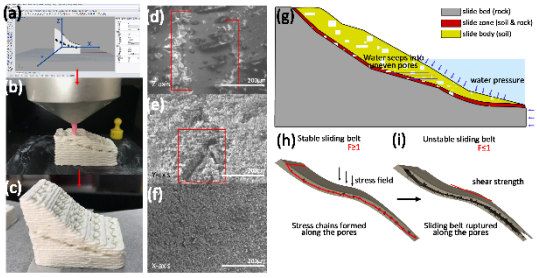


architecture printing is subject to harsh environmental examinations (such as high temperature, high pressure, weightlessness, etc.). In recent years, mars, moon and other outer space printing are explored and practiced more.[102, 103] Cesaretti et al. gave a complete introduction to the lunar soil printing process through a special binding liquid.[104] In order to resist the effects of radiation and temperature, a particular patented 3D-printing technology - D-shape- has assessed physical and chemical characteristics of lunar regolith and terrestrial regolith simulants. Meanwhile, Kading et al. had the same idea of utilizing in-situ resource sand 3D printing structures for a manned Mars mission.[105] This technical process used the printing of basalt and additives, and the printing process is divided into two stages: the construction of the

frame structure and the filling of the structure. In general, these are all environmentally friendly, which is very important for architecture construction.

### 4.2 Geological engineering model application

Precise simulation of topography and geomorphology models can reproduce, judge and simulate geological hazards. It's an inevitable trend in the long run because 3D printing of mineral materials can provide more accurate scaled-down models. Mineral material composites used for printing in the field of geological engineering applications are based on various types of mineral powder as well as binder to satisfy the mechanical properties of rock and soil.

To understand geomorphological activity and morphology such as mudslides and landslides, scientists commonly use simulations of physical models. Although the simulation of landform has not yet been able to achieve performance simulations, the structures is also crucial for understanding the topography. Hasiuk et al. thought that the model from image to reality is important for answering questions about Earth's history and making predictions about its future the evolution of the landscape in **Fig. 8**.[106]

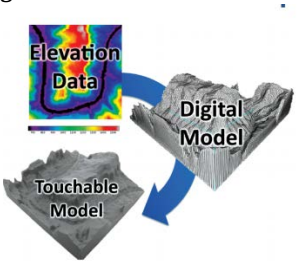


**Fig. 8** The journey from data to a tangible model through a touchable, 3D printed, touchable model **Ref. 106**

Recently, the simulation and printing of some landslide materials were developed.[8] The coordination of stress field and permeability in landslide models has been a problem that has not been well solved. During the development of the landslide model, new materials (liquid paraffin 3 wt. %, solid paraffin 12 wt. %, stearic acid 1.8 wt. %, palm wax 4.8 wt. % and barite powder 78.4%) were constantly developed to meet the requirements, while neglecting the effect of pores on the stress field and permeability during material formation. The group used a DIW technique to shape a small landslide model in **Fig. 9** that can achieve micron-scale models and a wider range of mechanical properties.

**Fig. 9** Manufacturing process of small model: (a) modeling process, (b) 3D printing, (c) forming of model. SEM images of model affected by process: process trace from (d) Z –axis, (e) Y-axis and (f) X-axis. (g) The rupture process of the sliding belt, (h) porous slip belt, (i) ruptured slip belt **Ref. 8**

### 4.3 Multi-functional micro components application

The performance improvement of micro- and nano-components has always been a concern, and the complex three-dimensional structure brought by DIW enhances the electrochemical performance. The micro-pore structure of mineral materials brings about better electrochemical performance and promotes the application of micro-functional components.[107] In particular, the printing of fossil fuel cells is the most studied. DIW significantly improves feature performance through holes design. In addition, the micro / nano-scale material forming is the main advantage of 3D printing, effectively improving the chemical properties.[108]

One of the important factors in the performance of functional micro parts is particle size effects. In the electrochemical cell, empty spaces and pores of the battery are filled with the electrolyte. Thus, whatever the size of these pores and spaces be lager, the ion transfer is easier and ion mass transfer resistance is smaller. Where the physical meaning of the three-dimensional structure of the electrode, fractal dimension of surfaces can be used as a factor for their porosity.

Recently, high-performance materials printing such as graphene battery printing is a frontier research. Dong et al. got a well-dispersed nanostructured battery through a solution immersion method.[10] Huang et al. reported the synthesis of MoO2 nanoparticles grown on three dimensional graphene (3DG) through a facile chemical vapor deposition (CVD) approach.[109] The latest research by Lacey et al. illustrated the importance of both porous nanomaterial and structurally conscious electrode designs (**Fig. 10**).[110] Compared to a 2D vacuum filtrated film, macroscale and porosity of the 3D printed mesh enhanced active-site utilization as well as mass/ionic transport to dramatically improve overall Li-$O_2$ battery performance (42-fold and 63-fold improvement in full discharge capacity by mass and area, respectively). Thus, this work demonstrates that conscious design and implementation of nanoporous carbon-based materials into hierarchically porous electrode architectures can enhance the performance of next-generation energy storage systems. Future research will inevitably expand the scope of integration of mineral materials with other new materials and give full play to the role of innovative materials and three-dimensional structures.

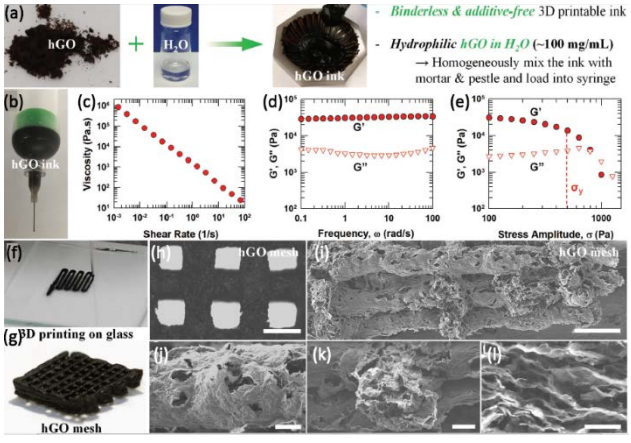


**Fig. 10** Extrusion-based 3D printed ink properties and hierarchically porous hGO mesh architecture. (a) Scheme showing the components

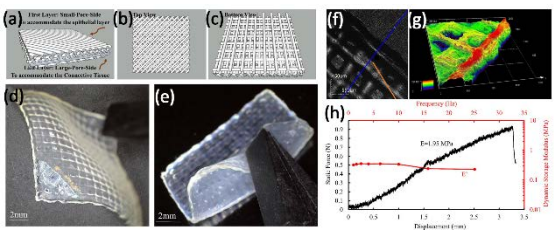


(hGO, $H_2O$) used to create the aqueous and additive-free 3D printable ink. (b) Digital image of the aqueous hGO ink loaded into a printing syringe. (c–e) Rheological properties of the hGO ink showing that the ink is solid-like at rest (i.e., has a yield stress) and exhibits shear-

thinning behavior with increasing shear. An estimate of the yield stress is obtained from the data in (d): $\sigma_y \approx 500$ Pa. (f) Digital image showing the process of printing complex 3D architectures line-by-line. (g) Isometric view of the printed hGO mesh (0.8 mm line spacing) after lyophilization. (h) Optical image showing a top-down view of the freeze-dried hGO mesh structure. Scale bar is 500 μm. (i) Cross-sectional SEM images of the hierarchically porous 3D printed hGO mesh structure: hGO sheets are nanoporous (4–25 nm holes), lyophilization creates tens of micrometer-sized pores on the printed filaments and the printed mesh structure possesses <500 μm square pores. Note that the hGO sheets are layered along the extruding direction due to the printing procedure, as shown in (l). Scale bars in (j) and (k) are 50 μm while (i) and (l) are 250 μm and 10 μm, respectively **Ref. 110**

### 4.4 Bio-mimic and Tissue scaffolds application

With the needs of the application of human tissue scaffolds, biomimetic stents for deposition-based 3D printed mineral material composites have emerged. On the one hand, mineral materials provide the requirements for mechanical properties and human compatibility.[111] On the other hand, 3D printing enables compatible design for many materials and complex structures. Mineral material composites used for printing in the field of architecture applications are based on muti-mineral as well as binder.[112] The design of minerals for biological applications is more quantitative than other applications.

The parameters of mineral fiber material have a decisive influence on the mechanical bearing capacity. Pores are varied in size and shape in the bracket, and they can be changed by changing fiber diameter, spacing and orientation, and layer thickness. Elastic properties such as dynamic stiffness and equilibrium modulus, and the viscous parameters like damping factor and creep unrecovered strain have regularity with pore structure design.

Tissue holder system control and deposition information are closely related. Pneumatic nozzles are more economical and precise control mechanisms in the printing of tissue supports. Because of the different concentrations of printed mineral materials, the stability of the flow rate requires the cooperation of various parameters.[113] Lobat et al printed the selected solution at material container temperature of 30–32 °C, platform temperature of 11 °C, printing pressure of 0.6–1.2 bar, speed of 20 mm/s using 250 μm-diameter needle.[114] As a result, six-layer membrane had good biocompatibility, desirable thickness (150 μm), static tensile modules (1.95 ± 0.55 M Pa) and dynamic tensile storage modulus (314 ± 50 K Pa) to enable easy surgical handling (**Fig. 11**). The ideal inlet pressure in most tissue bracket application is around 1 bar, and the dosing pressure on the market can reach 16-20 bar, such as the nozzle from ViscoTec LTD (vipro-HEAD3) which provides precise deposition positioning.

**Fig. 11** (a–c): Schematic of our design. Each membrane is composed of 6 layers. The strand angels from the first layer to the last layer are: 45, 135, 0, 90, 0, 90°. Distances between strands (from the middle of one strand to the middle of the adjacent one) are set to 0.6 μm for the layers 1–4 and 0.9 μm for layers 5–6. (d–e): The macroscopic view of the 3D-printed gradient membranes of gelatin/elastin/sodium hyaluronate. The membranes are completely flexible and bendable. The surgical handling of the membrane is easy. The thickness is approximately 150 μm. (f) The 3D laser imaging of the membranes to confirm the thickness of the membranes measured by the Electronic Digital Micrometer. (g) The height profile of the edge of the membrane. (h) Static mechanical testing revealed elastic modulus of 1.95 ± 0.55 M Pa (black); dynamic storage modulus vs. Frequency for printed membranes (red). The measured dynamic storage modulus was 314 ± 50 K Pa and had not been significantly altered by increasing the frequency. (For interpretation of the references to color in this figure legend, the reader is referred to the web version of this article.) **Ref. 113**

Compared with other forming methods, the multi-nozzle forming method can controlled amount of cells, growth factors, or other bioactive compounds with precise spatial position. Especially in the application of biological tissue, the new material can be used quickly and be easy to control the process. Yan et al designed a four-nozzle system to realize the bone support manufacturing process.[115] In the experiments, bone tissue engineering scaffolds with different properties were prepared using a single nozzle deposition process, a dual nozzle deposition process, and a three-nozzle deposition process, respectively. The bone scaffolds made in the deposition system had good biocompatibility and bone conductive property as a molecular scaffold, and it was used for bone morphogenic protein (BMP) in the implantation experiment of repairing segment defect of rabbit radius. The stability of injection extrusion is a major process challenge in the selection process of multi nozzle control. In the future development, although the demand for biological experiments is very inclusive, the accuracy requirement will gradually unify the technical standards for the design of the nozzles.

## 5. Conclusions

Although deposition-based 3D printed mineral material composites has undergone significant development in recent years, it is still not excavated and used by many industries. The technology still needs to break through several aspects and be more scientifically focused.

### 5.1 Material

Currently, deposition-based 3D printed materials are highly dependent on adhesives. Due to the high degree of freedom of the forming method, the compatibility of various mineral materials is strong. However, this also leads to the mutual influence of materials, making it difficult to achieve the required performance accuracy. The demand function achieved by one or more mineral materials is also affected by the performance of the additive without sintering. Therefore, it is necessary to avoid multiple mineral powders to achieve different functions. The development of composite mineral materials can effectively achieve precise positioning of performance and reduce material cost.

### 5.2 Process and Equipment

Multi-nozzle printing of mineral materials and other materials in 3D printing is a current research hot spot. When the mineral material is used as a functional material, it forms a complicated structure with other materials such as a polymer material, a biological material, etc. Double print heads or multi-head print systems coordinate the diversity of print components. Once it comes to printing with multiple print

heads, it becomes more difficult to control the movement of the parts and the material, resulting in a large gap in the viscosity characteristics of different mineral materials. As a result, the optimized design of the drive device and the spray head has become the focus of mechanical design.

### 5.3 Applications

Because there is no systematic study of the potential for deposition-based 3D printed mineral material composites, there are, as yet, few applications for the printing of mineral materials in many fields, and the application of this technology can achieve a breakthrough in traditional research. The awakening of future research may be in two directions. On the one hand, the application of biomimetic simulation may be achieved by combining the synchronous design of mineral materials and structures, which combines the simulation of shape and function. Another prospect lies in the use of mineral raw materials in situ because of the general trend of green manufacturing and will not be limited to construction.

As evidenced by the above-mentioned publications, researchers are exploring new materials and new application of deposition-based 3D printed mineral material composites. This paper gives a platform based on which further researchers will progress more. In terms of materials, processing control, product performance and applications, there are new avenues of research with 3D printing of polymer composites.

## ACKNOWLEDGEMENT

The project was kindly supported by the Fundamental Research Funds for the Central Universities, China University of Geosciences (Wuhan) (No.CUG170677). The authors also gratefully acknowledge the financial support from National Natural Science Foundation of China (No. 51675496, No. 51671091) and Wuhan Applied Basic Research Project, China (No. 2017010201010126)

## REFERENCES

1 Lewis, J.A., Smay, J.E., Stuecker, J., and Cesarano, J., “Direct Ink Writing of Three‐Dimensional Ceramic Structures,” Journal of the American Ceramic Society, Vol. 89, No. 12, pp. 3599-3609, 2010.

2 Lewis, J.A., “Direct Ink Writing of 3D Functional Materials,” Advanced Functional Materials, Vol. 16, No. 17, pp. 2193-2204, 2006.

3 Simon, J.L., Michna, S., Lewis, J.A., Rekow, E.D., Thompson, V.P., Smay, J.E., Yampolsky, A., Parsons, J.R., and Ricci, J.L., “In vivo bone response to 3D periodic hydroxyapatite scaffolds assembled by direct ink writing,” Journal of Biomedical Materials Research Part A, Vol. 83A, No. 3, pp. 747–758, 2007.

4 Fu, Q., Saiz, E., and Tomsia, A.P., “Direct Ink Writing of Highly Porous and Strong Glass Scaffolds for Load-bearing Bone Defects Repair and Regeneration,” Acta Biomaterialia, Vol. 7, No. 10, pp. 3547, 2011.

5 Bose, S., Vahabzadeh, S., and Bandyopadhyay, A., “Bone tissue engineering using 3D printing,” Materials Today, Vol. 16, No. 12, pp. 496-504, 2013.

6 Rajabi, J., Muhamad, N., Sulong, A.B., Fayyaz, A., and Wahi, A., “Advantages and Limitations of Using Nano Sized Powders for Powder Injection Molding Process: A Review,” Jurnal Teknologi, Vol. 59, No. 2, pp. 137-140, 2014.

7 Goulas, A., and Friel, R.J., “3D printing with moondust,” Rapid Prototyping Journal, Vol. 22, No. 6, pp. IN PRESS, 2015.

8 Tang, D., Hao, L., Li, Y., Xiong, W., Sun, T., and Yan, X., “Investigation of Wax-Based Barite Slurry and Deposition for 3D Printing Landslide Model,” Composites Part A Applied Science & Manufacturing, 2018.

9 Ahmad, F.N., Jaafar, M., Palaniandy, S., and Azizli, K.A.M., “Effect of particle shape of silica mineral on the properties of epoxy composites,” Composites Science & Technology, Vol. 68, No. 2, pp. 346-353, 2008.

10 Ji, D., Zhou, H., Tong, Y., Wang, J., Zhu, M., Chen, T., and Yuan, A., “Facile fabrication of MOF-derived octahedral CuO wrapped 3D graphene network as binder-free anode for high performance lithium-ion batteries,” Chemical Engineering Journal, 2016.

11 Yamashita, T., Yoshino, K., and Kaneko, A., “Micro/nano-mechanical structure fabricated by transfer printing,” International Journal of Precision Engineering & Manufacturing, Vol. 15, No. 12, pp. 2581-2587, 2014.

12 Chu, W.S., Kim, C.S., Lee, H.T., Choi, J.O., Park, J.I., Song, J.H., Jang, K.H., and Ahn, S.H., “Hybrid manufacturing in micro/nano scale: A Review,” International Journal of Precision Engineering and Manufacturing-Green Technology, Vol. 1, No. 1, pp. 75-92, 2014.

13 Kim, H.B., Hobler, G., Steiger, A., Lugstein, A., Bertagnolli, E., Platzgummer, E., and Loeschner, H., “Sputter-redeposition method for the fabrication of automatically sealed micro/nanochannel using FIBs,” International Journal of Precision Engineering & Manufacturing, Vol. 12, No. 5, pp. 893-898, 2011.

14 Khare, V., Sonkaria, S., Lee, G.-Y., Ahn, S.-H., and Chu, W.-S., “From 3D to 4D printing – design, material and fabrication for multi-functional multi-materials,” International Journal of Precision Engineering and Manufacturing-Green Technology, Vol. 4, No. 3, pp. 291-299, 2017.

15 Chu, W.-S., Kim, C.-S., Lee, H.-T., Choi, J.-O., Park, J.-I., Song, J.-H., Jang, K.-H., and Ahn, S.-H., “Hybrid manufacturing in micro/nano scale: A Review,” International Journal of Precision Engineering and Manufacturing-Green Technology, Vol. 1, No. 1, pp. 75-92, 2014.

16 Yi, H., Hwang, I., Sung, M., Lee, D., Kim, J.H., Kang, S.M., Bae, W.G., and Jeong, H.E., “Bio-inspired adhesive systems for next-generation green manufacturing,” International Journal of Precision Engineering and Manufacturing-Green Technology, Vol. 1, No. 4, pp. 347-351, 2014.

17 Ho, C.M.B., Ng, S.H., and Yoon, Y.J., “A review on 3D printed

bioimplants," International Journal of Precision Engineering & Manufacturing, Vol. 16, No. 5, pp. 1035-1046, 2015.

18 Sa, M.W., and Kim, J.Y., "Effect of various blending ratios on the cell characteristics of PCL and PLGA scaffolds fabricated by polymer deposition system," International Journal of Precision Engineering & Manufacturing, Vol. 14, No. 4, pp. 649-655, 2013.

19 Hong-Mei, H.U., and Bao-Guo, M.A., "Experiment study on mineral functional materials in improving chloride ion penetration of concrete," Concrete, 2004.

20 Nakanishi, K., "Quartz plate and quartz resonator in which the quartz plate is used, 2015.

21 Ma, J., Tang, H., Hu, X., Bobet, A., Yong, R., and Eldin, M.A.M.E., "Model testing of the spatial–temporal evolution of a landslide failure," Bulletin of Engineering Geology & the Environment, Vol. 76, No. 1, pp. 1-17, 2016.

22 Adamu, M., Mohammed, B.S., and Shafiq, N., "Effect of Polycarboxylate Superplasticizer Dosage on the Mechanical Performance of Roller Compacted Rubbercrete for Pavement Applications," Journal of Engineering & Applied Science, Vol. 12, No. 20, pp. 5253-5260, 2017.

23 Larisa, U., Solbon, L., and Sergei, B., "Fiber-reinforced Concrete with Mineral Fibers and Nanosilica," Procedia Engineering, Vol. 195, pp. 147-154, 2017.

24 Egorov, A.A., Fedotov, A.Y., Mironov, A.V., Komlev, V.S., Popov, V.K., and Zobkov, Y.V., "3D printing of mineral-polymer bone substitutes based on sodium alginate and calcium phosphate," Beilstein Journal of Nanotechnology, Vol. 7, No. 1, pp. 1794, 2016.

25 Fedotov, A.Y., Egorov, A.A., Zobkov, Y.V., Mironov, A.V., Popov, V.K., Barinov, S.M., and Komlev, V.S., "3D printing of mineral-polymer structures based on calcium phosphate and polysaccharides for tissue engineering," Inorganic Materials Applied Research, Vol. 7, No. 2, pp. 240-243, 2016.

26 Shah, A.U.R., Prabhakar, M.N., and Song, J.-I., "Current advances in the fire retardancy of natural fiber and bio-based composites – A review," International Journal of Precision Engineering and Manufacturing-Green Technology, Vol. 4, No. 2, pp. 247-262, 2017.

27 Ahn, D.-G., "Direct metal additive manufacturing processes and their sustainable applications for green technology: A review," International Journal of Precision Engineering and Manufacturing-Green Technology, Vol. 3, No. 4, pp. 381-395, 2016.

28 Chen, H., Xu, Q., Chen, S., and Zhang, Z., "Evaluation and design of fiber-reinforced asphalt mixtures," Materials & Design, Vol. 30, No. 7, pp. 2595-2603, 2009.

29 Fratzl, P., Gupta, H.S., Paschalis, E.P., and Roschger, P., "Structure and mechanical quality of the collagen–mineral nano-composite in bone," Journal of Materials Chemistry, Vol. 14, No. 14, pp. 2115-2123, 2004.

30 Yazıcı, H., Yardımcı, M.Y., Aydın, S., and Karabulut, A.Ş., "Mechanical properties of reactive powder concrete containing mineral admixtures under different curing regimes," Construction & Building Materials, Vol. 23, No. 3, pp. 1223-1231, 2009.

31 Puget, P., Chenu, C., and Balesdent, J., "Dynamics of soil organic matter associated with particle-size fractions of water-stable aggregates," European Journal of Soil Science, Vol. 51, No. 4, pp. 595-605, 2000.

32 Baldock, J.A., and Skjemstad, J.O., "Role of the soil matrix and minerals in protecting natural organic materials against biological attack," Organic Geochemistry, Vol. 31, No. 7, pp. 697-710, 2000.

33 Corinaldesi, V., and Moriconi, G., "Durable fiber reinforced self-compacting concrete," Cement & Concrete Research, Vol. 34, No. 2, pp. 249-254, 2004.

34 Szabó, J.S., and Czigány, T., "Static fracture and failure behavior of aligned discontinuous mineral fiber reinforced polypropylene composites," Polymer Testing, Vol. 22, No. 6, pp. 711-719, 2003.

35 Tai, Y.S., Pan, H.H., and Kung, Y.N., "Mechanical properties of steel fiber reinforced reactive powder concrete following exposure to high temperature reaching 800 °C," Nuclear Engineering & Design, Vol. 241, No. 7, pp. 2416-2424, 2011.

36 Bijwe, J., "Composites as friction materials: Recent developments in non‐asbestos fiber reinforced friction materials—a review," Polymer Composites, Vol. 18, No. 3, pp. 378-396, 1997.

37 Lee, C.-M., Woo, W.-S., and Roh, Y.-H., "Remanufacturing: Trends and issues," International Journal of Precision Engineering and Manufacturing-Green Technology, Vol. 4, No. 1, pp. 113-125, 2017.

38 Elshafie, S., Boulbibane, M., and Whittleston, G., "Influence of Mineral Admixtures on the Mechanical Properties of Fresh and Hardened Concrete," Construction Science, Vol. 19, No. 1, 2017.

39 Singh, S., Ransinchung, G.D., and Kumar, P., "Effect of mineral admixtures on fresh, mechanical and durability properties of RAP inclusive concrete," Construction & Building Materials, Vol. 156, pp. 19-27, 2017.

40 Li, W., and Xu, J., "Mechanical properties of basalt fiber reinforced geopolymeric concrete under impact loading," Materials Science & Engineering A, Vol. 505, No. 1, pp. 178-186, 2009.

41 Pickering, S.J., "Recycling technologies for thermoset composite materials—current status," Composites Part A Applied Science & Manufacturing, Vol. 37, No. 8, pp. 1206-1215, 2006.

42 Wang, W., Song, J., Yan, B., and Yu, Y., "Metal injection molding of tungsten and its alloys," Metal Powder Report, Vol. 71, No. 6, 2016.

43 Dehghan-Manshadi, A., Bermingham, M., Dargusch, M., Stjohn, D., and Ma, Q., "Metal Injection Moulding of Titanium and Titanium Alloys: Challenges and Recent Development," Powder Technology, 2017.

44 Rueschhoff, L.M., Trice, R.W., and Youngblood, J.P., "Near-net shaping of silicon nitride via aqueous room-temperature injection molding and pressureless sintering," Ceramics International, Vol. 43, No. 14, 2017.

45 Han, J.S., Chang, W.G., Park, J.M., and Park, S.J., "Powder

injection molding of PNN-PMN-PZN doped low temperature sintering PZT ceramics," Journal of Manufacturing Processes, Vol. 28, pp. 235-242, 2017.

46 Zaky, M.T., Soliman, F.S., and Farag, A.S., "Influence of paraffin wax characteristics on the formulation of wax-based binders and their debinding from green molded parts using two comparative techniques," Journal of Materials Processing Tech, Vol. 209, No. 18, pp. 5981-5989, 2009.

47 Wang, Y.E., Han, Q., Wei, S.M., Li, P.L., Yang, M.M., Qin, Y.L., Wang, Y.B., and Zhou, J.H., "Analysis to Effective Elastic Modulus and Porosity for Artificial Bone Scaffold with Hydroxyapatite Microspheres," Advanced Materials Research, Vol. 424-425, pp. 241-245, 2012.

48 Li, C., Wu, J., Tang, H., Hu, X., Liu, X., Wang, C., Liu, T., and Zhang, Y., "Model testing of the response of stabilizing piles in landslides with upper hard and lower weak bedrock," Engineering Geology, Vol. 204, pp. 65-76, 2016.

49 Kumar, P., Rodrigues, H.J., Ds, L., Hubaish, M., and G, B., "Design and fabrication of powder based binder jetting 3D printing," Ceramics International, Vol. 3, No. 9, pp. 142-150, 2017.

50 Zafar, A., Schjødt-Thomsen, J., Sodhi, R., Goacher, R., and Kubber, D.D., "Investigation of the ageing effects on phenol-urea-formaldehyde binder and alkanol amine-acid anhydride binder coated mineral fibres," Polymer Degradation & Stability, Vol. 98, No. 1, pp. 339-347, 2013.

51 Wang, J., Calhoun, M.D., and Severtson, S.J., "Dynamic rheological study of paraffin wax and its organoclay nanocomposites," Journal of Applied Polymer Science, Vol. 108, No. 4, pp. 2564–2570, 2008.

52 Luyt, A.S., and Geethamma, V.G., "Effect of oxidized paraffin wax on the thermal and mechanical properties of linear low-density polyethylene–layered silicate nanocomposites," Polymer Testing, Vol. 26, No. 4, pp. 461-470, 2007.

53 Miyanaji, H., Li, Y., Zhang, S., and Zandinejad, A.: "A preliminary study of the graded dental porcelain ceramic structures fabricated via binder jetting 3D printing," in Editor (Ed.)^(Eds.): "Book A preliminary study of the graded dental porcelain ceramic structures fabricated via binder jetting 3D printing" (2014, edn.), pp.

54 Hansen, E.L., "Aqueous binder composition for mineral fibers, 2012.

55 Trunec, M., and Cihlar, J., "Thermal removal of multicomponent binder from ceramic injection mouldings," Journal of the European Ceramic Society, Vol. 22, No. 13, pp. 2231-2241, 2002.

56 Oliveira, R.V.B., Soldi, V., Fredel, M.C., and Pires, A.T.N., "Ceramic injection moulding: influence of specimen dimensions and temperature on solvent debinding kinetics," Journal of Materials Processing Tech, Vol. 160, No. 2, pp. 213-220, 2005.

57 Rueschhoff, L., Costakis, W., Michie, M., Youngblood, J., and Trice, R., "Additive Manufacturing of Dense Ceramic Parts via Direct Ink Writing of Aqueous Alumina Suspensions," International Journal of Applied Ceramic Technology, Vol. 13, No. 5, pp. 821-830, 2016.

58 Kafara, M., Kemnitzer, J., Westermann, H.H., and Steinhilper, R., "Influence of Binder Quantity on Dimensional Accuracy and Resilience in 3D-Printing," Procedia Manufacturing, Vol. 21, pp. 638-646, 2018.

59 Sun, Z., Qin, M., Li, R., Ma, J., Fang, F., Lu, H., and Qu, X., "Preparation of high performance soft magnetic alloy Fe-4Si-0.8P by metal injection molding," Advanced Powder Technology, 2017.

60 Kate, K.H., Enneti, R.K., Mccabe, T., and Atre, S.V., "Simulations and injection molding experiments for aluminum nitride feedstock," Ceramics International, Vol. 42, No. 1, pp. 194-203, 2016.

61 Peltola, P., Välipakka, E., Vuorinen, J., Syrjälä, S., and Hanhi, K., "Effect of rotational speed of twin screw extruder on the microstructure and rheological and mechanical properties of nanoclay-reinforced polypropylene nanocomposites," Polymer Engineering & Science, Vol. 46, No. 8, pp. 995–1000, 2006.

62 Gomes, C.M., Travitzky, N., Greil, P., Oliveira, A.P.N., and Hotza, D., "Laminated Object Manufacturing (LOM) of glass ceramics substrates for LTCC applications, 2010.

63 Ning, F., Cong, W., Qiu, J., Wei, J., and Wang, S., "Additive manufacturing of carbon fiber reinforced thermoplastic composites using fused deposition modeling," Composites Part B Engineering, Vol. 80, pp. 369-378, 2015.

64 Mireles, J., Kim, H.C., Lee, I.H., Espalin, D., Medina, F., Macdonald, E., and Wicker, R., "Development of a Fused Deposition Modeling System for Low Melting Temperature Metal Alloys," Journal of Electronic Packaging, Vol. 135, No. 1, pp. 011008, 2013.

65 Hao, L., Seaman, O., Mellor, S., Henderson, J., Sewell, N., and Sloan, M., "Extrusion behavior of chocolate for additive layer manufacturing, 2010.

66 Submitted, A.D., The, F.O.R., Of, D., and Of, D., "Process Parameter Optimization for Direct Metal Laser Sintering (DMLS)," Ph D, 2005.

67 Parthasarathy, J., Starly, B., Raman, S., and Christensen, A., "Mechanical evaluation of porous titanium (Ti6Al4V) structures with electron beam melting (EBM)," J Mech Behav Biomed Mater, Vol. 3, No. 3, pp. 249-259, 2010.

68 Russias, J., Cardinal, S., Esnouf, C., Fantozzi, G., and Bienvenu, K., "Hot pressed titanium nitride obtained from SHS starting powders: Influence of a pre-sintering heat-treatment of the starting powders on the densification process," Journal of the European Ceramic Society, Vol. 27, No. 1, pp. 327-335, 2007.

69 Wang, X.C., Laoui, T., Bonse, J., Kruth, J.P., Lauwers, B., and Froyen, L., "Direct Selective Laser Sintering of Hard Metal Powders: Experimental Study and Simulation," International Journal of Advanced Manufacturing Technology, Vol. 19, No. 5, pp. 351-357, 2002.

70 Ganci, M., Zhu, W., Buffa, G., Fratini, L., Bo, S., and Yan, C., "A macroscale FEM-based approach for selective laser sintering of thermoplastics," International Journal of Advanced Manufacturing

Technology, Vol. 91, No. 9-12, pp. 1-12, 2017.

71 Zhao, J., Cao, W.B., Li, J.T., Han, Z., Li, Y.H., and Ge, C.C., "Selective Laser Sintering of $Si_3N_4$ and $Al_2O_3$ Ceramic Powders," Key Engineering Materials, Vol. 368-372, pp. 858-861, 2008.

72 Mizuno, J., and Takahashi, S., "A Double-Sided In-Plane Lateral Comb-Drive Actuator Fabricated by a Plaster-Based 3D-Printer," Key Engineering Materials, Vol. 656-657, pp. 594-599, 2015.

73 Mcfarland, C., Ahern, R., Nguyen, V., and Ayllon, R., "Stereolithography Apparatus (SLA) Prototype Part Tolerance Improvement, 2009.

74 Tyge, E., Pallisgaard, J.J., Lillethorup, M., Hjaltalin, N.G., Thompson, M.K., and Clemmensen, L.H., "Characterizing Digital Light Processing (DLP) 3D Printed Primitives, Vol. 9127, pp. 302-313, 2015.

75 Liao, Y.S., Chiu, L.C., and Chiu, Y.Y., "A new approach of online waste removal process for laminated object manufacturing (LOM)," Journal of Materials Processing Technology, Vol. 140, No. 1–3, pp. 136-140, 2003.

76 Prechtl, M., Otto, A., and Geiger, M., "Rapid Tooling by Laminated Object Manufacturing of Metal Foil," Advanced Materials Research, Vol. 6-8, pp. 303-312, 2005.

77 Tang, H., Hu, X., Xu, C., Li, C., Yong, R., and Wang, L., "A novel approach for determining landslide pushing force based on landslide-pile interactions," Engineering Geology, Vol. 182, pp. 15-24, 2014.

78 Kwon, J., Park, H.W., Park, Y.-B., and Kim, N., "Potentials of additive manufacturing with smart materials for chemical biomarkers in wearable applications," International Journal of Precision Engineering and Manufacturing-Green Technology, Vol. 4, No. 3, pp. 335-347, 2017.

79 Sharma, A., Mondal, S., Mondal, A.K., Baksi, S., Patel, R.K., Chu, W.-S., and Pandey, J.K., "3D printing: It's microfluidic functions and environmental impacts," International Journal of Precision Engineering and Manufacturing-Green Technology, Vol. 4, No. 3, pp. 323-334, 2017.

80 Ly, S.T., and Kim, J.Y., "4D printing – fused deposition modeling printing with thermal-responsive shape memory polymers," International Journal of Precision Engineering and Manufacturing-Green Technology, Vol. 4, No. 3, pp. 267-272, 2017.

81 Moon, S.K., Tan, Y.E., Hwang, J., and Yoon, Y.-J., "Application of 3D printing technology for designing light-weight unmanned aerial vehicle wing structures," International Journal of Precision Engineering and Manufacturing-Green Technology, Vol. 1, No. 3, pp. 223-228, 2014.

82 Woodfield, T.B.F., Malda, J., Wijn, J.D., Péters, F., Riesle, J., and Blitterswijk, C.A.V., "Design of porous scaffolds for cartilage tissue engineering using a three-dimensional fiber-deposition technique," Biomaterials, Vol. 25, No. 18, pp. 4149-4161, 2004.

83 Treppo, S., Koepp, H., Quan, E.C., Cole, A.A., Kuettner, K.E., and Grodzinsky, A.J., "Comparison of biomechanical and biochemical properties of cartilage from human knee and ankle pairs," Journal of Orthopaedic Research, Vol. 18, No. 5, pp. 739-748, 2000.

84 Eftekhari, A., "3D Deposition of $LiMn_2O_4$: enhancement of lithium battery performance," Solid State Ionics, Vol. 161, No. 1–2, pp. 41-47, 2003.

85 Xie, J., Harks, P.P.R.M.L., Li, D., Raijmakers, L.H.J., and Notten, P.H.L., "Planar and 3D deposition of Li 4 Ti 5 O 12 thin film electrodes by MOCVD," Solid State Ionics, Vol. 287, pp. 83-88, 2016.

86 Gaal, G., Mendes, M., Almeida, T.P.D., Piazzetta, M.H.O., Gobbi, Â.L., Jr, A.R., and Rodrigues, V., "Simplified fabrication of integrated microfluidic devices using fused deposition modeling 3D printing," Sensors & Actuators B Chemical, Vol. 242, pp. 35-40, 2017.

87 Choi, J.H., Lee, S., and Lee, J.W., "Non-Newtonian behavior observed via dynamic rheology for various particle types in energetic materials and simulant composites," Korea-Australia Rheology Journal, Vol. 29, No. 1, pp. 9-15, 2017.

88 Russel, W.B., Saville, D.A., and Schowalter, W.R., "Colloidal Dispersion, Vol. 37, No. 5, pp. 14185-14192, 1981.

89 Elimelech, M., Jia, X., Gregory, J., and Williams, R., "Particle Deposition and Aggregation," Particle Deposition & Aggregation, Vol. 88, No. 6, pp. xiii–xv, 1998.

90 Shrotri, S., and Somasundaran, P., "Particle deposition and aggregation, measurement, modeling and simulation," Colloids & Surfaces A Physicochemical & Engineering Aspects, Vol. 125, No. 1, pp. 93–94, 1997.

91 Le-Hua, Chao, Luo, Y.P., Zhou, J., Hou, J.M., Li, X.H., and He-Jun, "A novel selection method of scanning step for fabricating metal components based on micro-droplet deposition manufacture," International Journal of Machine Tools & Manufacture, Vol. 56, No. 2, pp. 50-58, 2012.

92 Bell, L., "Top-Level Considerations for Planning Lunar/Planetary Habitat Structures," Journal of Aerospace Engineering, Vol. 24, No. 3, pp. 349-360, 2011.

93 Nair, G.M., Murthi, K.R.S., and Prasad, M.Y.S., "Strategic, technological and ethical aspects of establishing colonies on Moon and Mars," Acta Astronautica, Vol. 63, No. 11–12, pp. 1337-1342, 2008.

94 Castilho, M., Moseke, C., Ewald, A., Gbureck, U., Groll, J., Pires, I., Teßmar, J., and Vorndran, E., "Direct 3D powder printing of biphasic calcium phosphate scaffolds for substitution of complex bone defects," Biofabrication, Vol. 6, No. 1, pp. 015006, 2014.

95 Luo, Y., Li, Y., Qin, X., and Wa, Q., "3D printing of concentrated alginate/gelatin scaffolds with homogeneous nano apatite coating for bone tissue engineering," Materials & Design, 2018.

96 Kokkinis, D., Bouville, F., and Studart, A.R., "3D Printing of Materials with Tunable Failure via Bioinspired Mechanical Gradients," Advanced Materials, Vol. 30, No. 19, pp. 1705808, 2018.

97 Chang, Y., Shih, Y.J., Lai, C.J., Kung, H.H., and Jiang, S., "Blood‐Inert Surfaces via Ion‐Pair Anchoring of Zwitterionic

Copolymer Brushes in Human Whole Blood," Advanced Functional Materials, Vol. 23, No. 9, pp. 1100–1110, 2013.

98 Perrot, A., Rangeard, D., and Pierre, A., "Structural built-up of cement-based materials used for 3D-printing extrusion techniques," Materials & Structures, Vol. 49, No. 4, pp. 1213-1220, 2016.

99 Rangel, D.P., Superak, C., Bielschowsky, M., Farris, K., Falconer, R.E., and Baveye, P.C., "Rapid Prototyping and 3-D Printing of Experimental Equipment in Soil Science Research," Soil Science Society of America Journal, Vol. 77, No. 1, pp. 54-59, 2013.

100 Compton, B.G., and Lewis, J.A., "3D Printing: 3D‐Printing of Lightweight Cellular Composites," Advanced Materials, Vol. 26, No. 34, pp. 6043, 2014.

101 Bos, F., Wolfs, R., Ahmed, Z., and Salet, T., "Additive manufacturing of concrete in construction: potentials and challenges of 3D concrete printing," Virtual & Physical Prototyping, Vol. 11, No. 3, pp. 209-225, 2016.

102 SongJinghua, and ZhouQing, "3D Printing Technology for a Moon Outpost Exploiting Lunar Soil," Huazhong Architecture, 2015.

103 Matula, T., and Greene, K.A.: "Applying a Design-to-Evolve Approach to Early Lunar Settlements," in Editor (Ed.)^(Eds.): "Book Applying a Design-to-Evolve Approach to Early Lunar Settlements" (2014, edn.), pp. 1448-1457

104 Cesaretti, G., Dini, E., Kestelier, X.D., Colla, V., and Pambaguian, L., "Building components for an outpost on the Lunar soil by means of a novel 3D printing technology," Acta Astronautica, Vol. 93, No. 1, pp. 430-450, 2014.

105 Kading, B., and Straub, J., "Utilizing in-situ resources and 3D printing structures for a manned Mars mission," Acta Astronautica, Vol. 107, pp. 317-326, 2015.

106 Hasiuk, F., and Harding, C., "Touchable topography: 3D printing elevation data and structural models to overcome the issue of scale," Geology Today, Vol. 32, No. 1, pp. 16-20, 2016.

107 Sullivan, K.T., Zhu, C., Tanaka, D.J., Kuntz, J.D., Duoss, E.B., and Gash, A.E., "Electrophoretic Deposition of Thermites onto Micro-Engineered Electrodes Prepared by Direct-Ink Writing," Journal of Physical Chemistry B, Vol. 117, No. 6, pp. 1686-1693, 2013.

108 Chen, B., Jiang, Y., Tang, X., Pan, Y., and Hu, S., "Fully Packaged Carbon Nanotube Supercapacitors by Direct Ink Writing on Flexible Substrates," Acs Applied Materials & Interfaces, Vol. 9, No. 34, 2017.

109 Huang, Z.X., Wang, Y., Zhu, Y.G., Shi, Y., Wong, J.I., and Yang, H.Y., "3D graphene supported MoO2 for high performance binder-free lithium ion battery," Nanoscale, Vol. 6, No. 16, pp. 9839-9845, 2014.

110 Lacey, S.D., Kirsch, D.J., Li, Y., Morgenstern, J.T., Zarket, B.C., Yao, Y., Dai, J., Garcia, L.Q., Liu, B., and Gao, T., "Extrusion-Based 3D Printing of Hierarchically Porous Advanced Battery Electrodes," Advanced Materials, pp. 1705651, 2018.

111 Fiocco, L., Elsayed, H., Badocco, D., Pastore, P., Bellucci, D., Cannillo, V., Detsch, R., Boccaccini, A., and Bernardo, E., "Direct ink writing of silica-bonded calcite scaffolds from preceramic polymers and fillers," Biofabrication, Vol. 9, No. 2, pp. 025012, 2017.

112 Zocca, A., Franchin, G., Elsayed, H., Gioffredi, E., Bernardo, E., and Colombo, P., "Direct Ink Writing of a Preceramic Polymer and Fillers to Produce Hardystonite (Ca2ZnSi2O7) Bioceramic Scaffolds," Journal of the American Ceramic Society, Vol. 99, No. 6, pp. 1960-1967, 2016.

113 Khalil, S., Nam, J., and Sun, W., "Multi‐nozzle deposition for construction of 3D biopolymer tissue scaffolds," Rapid Prototyping Journal, Vol. volume 11, No. 1, pp. 9-17(19), 2005.

114 Tayebi, L., Rasoulianboroujeni, M., Moharamzadeh, K., Almela, T.K.D., Cui, Z., and Ye, H., "3D-printed membrane for guided tissue regeneration," Materials Science & Engineering C, Vol. 84, pp. 148-158, 2018.

115 Yan, Y., Xiong, Z., Hu, Y., Wang, S., Zhang, R., and Zhang, C., "Layered manufacturing of tissue engineering scaffolds via multi-nozzle deposition," Materials Letters, Vol. 57, No. 18, pp. 2623-2628, 2003.